

Lasers in Manufacturing Conference 2023

Laser drilling of high-density micro-holes on metals using a 1064nm nanosecond pulsed fibre laser

Themistoklis Karkantonis^{a,*}, Etienne Pelletier^a, Toby Barnard^a, Simon Tuohy^a,
Dimitris Karnakis^a

^a*Oxford Lasers Ltd, Unit 8 Moorbrook Park, Didcot OX11 7HP, United Kingdom*

Abstract

High-precision laser drilled micro-holes are ubiquitously found in industrial manufacturing, e.g. fuel-injectors, mesh filters, micro-dies, with a pressing need to cost-effectively scale up their production. For lasers to displace other established manufacturing technologies, high production throughput and yield are necessary which require the use of high-average-power lasers. Nanosecond pulsed fibre lasers offer an attractive choice to meet this challenge as they provide high-average-power without requiring capital intensive purchase or operation. However, unwanted thermal effects accompany their use, e.g. residual substrate heating, hole crater dross, hindering their wider adoption in high-precision applications. Here, we study high-density 1064nm fibre laser percussion drilling of 300 μm thick stainless-steel (exit hole diameters of 27 – 43 μm , pitch distance range 200 – 500 μm) by utilising the otherwise unwanted laser heat accumulation to improve drill speeds. Effective beam scanning strategies are coupled with thermal imaging to minimise any dimensional hole variations from residual heating, whilst aiming to monetise hole quality gains from progressively lower laser-induced temperature gradients in the gradually heated substrate. The results demonstrate the effectiveness of the proposed method in counteracting heat-induced side effects and consequently improving the overall laser drilling performance.

Keywords: Nanosecond fibre lasers; high-density holes; percussion laser drilling; heat accumulation

1. Introduction

Recent technological developments in various industrial sectors, e.g. aerospace, automotive, fluidics and filtration, have driven the demand for producing highly precise components with microscale features (Chaubey

* Corresponding author. Tel.: +44 (0) 1235 810088.

E-mail address: themis.karkantonis@oxfordlasers.com 01235 810088

et al., 2022; Nasrollahi et al., 2020). Many of these devices incorporate micro-holes, and thus laser drilling processes have received significant attention from both research and industrial communities. Owing to the intrinsic shortcomings of traditional manufacturing technologies, advanced micro-drilling techniques are usually deployed to fabricate such holes. Compared to other contactless processes, laser drilling is an attractive alternative as it offers high productivity, precision and also 3D processing capabilities (Piqué et al., 2016).

Generally, the use of ultrashort pulsed lasers is preferred in drilling applications where surface quality and integrity are valued higher than throughput. However, the relatively low material removal rates together with the very high operating costs associated with these lasers limit their broader industrial adoption (Karkantonis et al., 2022). On the contrary, nanosecond pulsed lasers with high-average-powers are already available to the market and are far less capital intensive (Dondieu et al., 2020). As a result, this technology is well-established in industrial production processes for many years now (Knowles et al., 2007). The primary concern when employing such laser sources for high-speed percussion drilling of metals is the heat accumulated by successive incident laser pulses. Although a moderate local temperature increase can improve ablation efficiency, uncontrolled heat accumulation can lead to both poor hole quality (i.e. extensive surface oxidation and recast formation) and poor drilling uniformity (Franz et al., 2022; Wang et al., 2018). Consequently, most nanosecond laser drilling operations require laborious post-processing steps to improve surface quality, e.g. electropolishing. Therefore, it is essential to introduce strategies that can mitigate such undesired laser-induced thermal effects.

To date, two main methods have been proposed to overcome heat accumulation side effects in laser percussion drilling operations while utilising the maximum average power of a given laser system. The first approach uses laser beam splitting technology to utilise parallel laser processing with multiple beamlets on target (Amako et al., 2016). Each beamlet can be tuned to carry an optimal laser power. In this case, a maximal average power available from the laser source can be used to drill multiple holes simultaneously. Nevertheless, these operations require a further investment in beam delivery and are complex to set up. The second approach requires the use of fast laser scanning, e.g. galvanometer or polygon scanners equipped with suitable focusing optics, to deflect the laser beam over the surface at high speeds and utilise high laser repetition rates (Rößler et al., 2020). Especially with polygon scanners which are well suited to mode-locked lasers, the area to be processed is divided into layers in the vertical direction based on the total number of laser pulses necessary to drill through the substrate. Then, it is scanned layer by layer to remove a small amount of material in every cycle by irradiating each hole with one pulse. Since scanners tend to have low positioning repeatability at high processing speeds, it is really challenging to deliver the laser pulses precisely enough at the same location in every repeated layer. At the same time, multi-layer laser drilling processes are not efficient as they involve many repeat cycles and also fail to utilise photoincubation effects both of which lead to reduced material removal rates.

Therefore, this research reports an alternative, more efficient method to enable nanosecond laser percussion drilling of high-density holes on metal foils without compromising the overall process uniformity and productivity. First, we show the influence of critical laser processing parameters on hole size and drilling rate. Thereafter, the heat accumulation effects are investigated using two scanning strategies, namely “*sequential*” and “*2D interlaced*”. Using evidence gained by thermal imaging, a strategy to counteract the negative thermal effects induced by such lasers is proposed and demonstrated.

2. Experimental procedures

ASTM A304 stainless steel (SS) rectangular sheets with a 300 μm thickness were used in this study. The pristine material was used as received and to remove any residual laser debris, the processed substrates were ultrasonically cleaned in deionised water for an hour immediately after laser drilling. The laser drilling

experiments were carried out on a high-power laser micro-machining workstation under ambient conditions, and its main component technologies are depicted in Fig. 1(a). The system integrates a 70 W nanosecond fibre laser source (EP-Z G4, SPI) that operates at a nominal wavelength of 1064 nm and pulse repetition rates of up to 1 MHz. The employed laser source incorporates pulse tune technology and hence it can deliver pulses of different duration, shape and energy. Since high throughput was targeted, only three of those that can provide a maximum pulse energy of 1 mJ were considered in this research, i.e. pulse durations of 240, 620 and 1020 ns.

Moreover, the optical beam delivery setup includes a beam collimator and a coaxial camera to monitor the drilling progress. A galvo scan head (excelliSCAN 14, SCANLAB) was used to deflect the laser beam at a maximum speed of 2000 mm/s, which was mounted on a linear Z motorised stage (L-812 series, Physik Instrumente). A telecentric lens with 163 mm focal length was integrated that resulted with input beam diameter 7.5 mm ($1/e^2$) in a focused laser spot size ($2w_0$) of 38 μm at the focal plane. The Rayleigh length was 1.03 mm. Linear XY motorized stages (V-817 series, Physik Instrumente) together with a height sensor (LK-G82, KEYENCE) were deployed to accurately position the laser post on the sample surface within the lens field of view. Finally, a CAD/CAM software (Direct Machining Control), was used to create the laser drilling recipes and generate the beam toolpath trajectories.

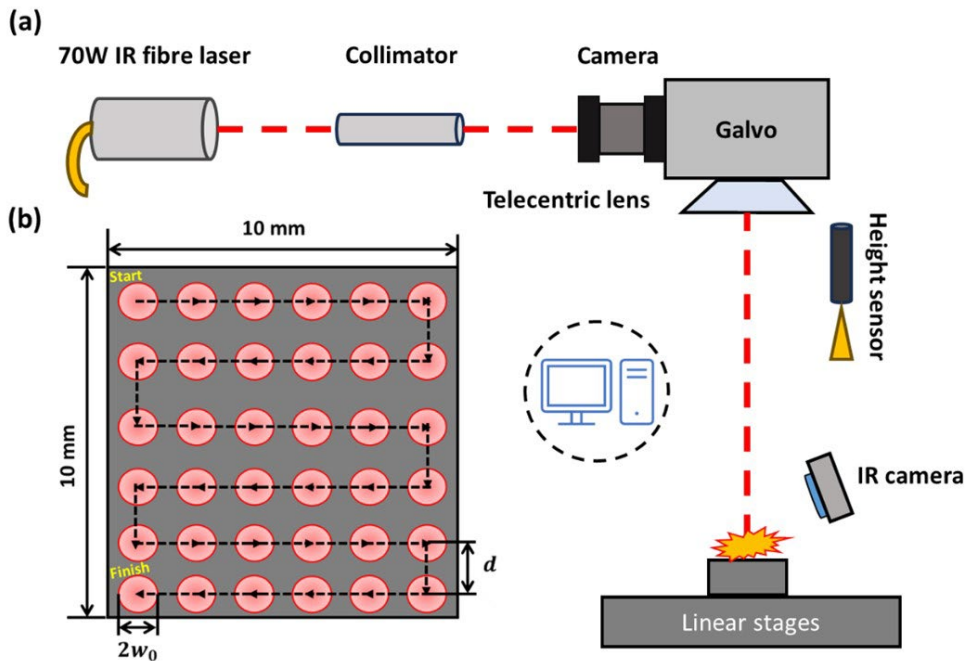


Fig. 1. Schematic representation of (a) the employed experimental laser setup and (b) the sequential scanning strategy used for hole drilling.

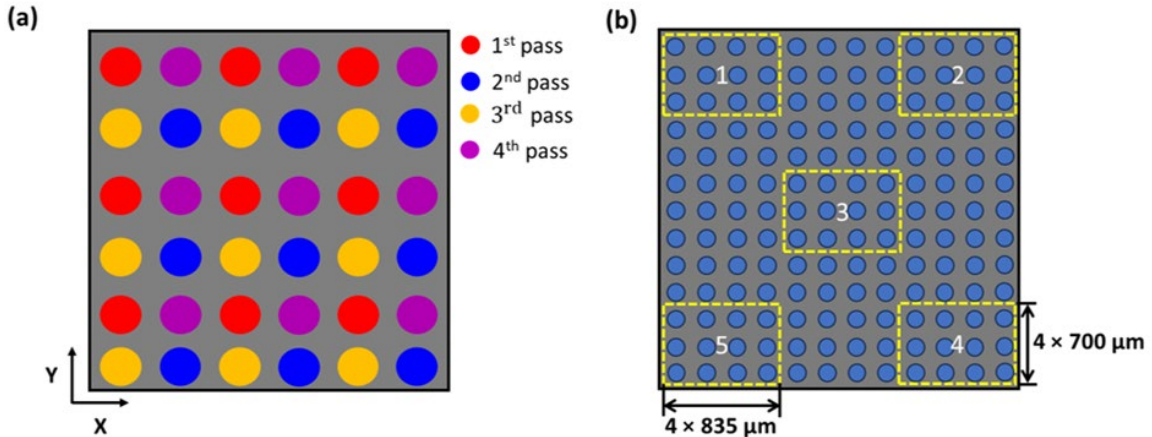


Fig. 2. Schematic illustration of (a) the 2D interlaced scanning method used to drill the array of holes showing indicatively four repeat passes and (b) the locations of test drilled holes measured on each processed SS substrate.

Initially, single holes were drilled on the SS surface to investigate the influence of critical laser processing parameters, such as laser pulse energy, repetition rate, pulse duration and number of laser pulses, on their dimensional characteristics. These holes are then used as reference to assess heat accumulation effects. The whole experimental procedure was repeated five times. Furthermore, high-density holes were drilled over a surface area of $10 \times 10 \text{ mm}^2$ by using a bidirectional sequential scanning strategy as illustrated in Fig. 1(b). In the employed strategy, the hole pitch distance (d) was varied from 200 to 500 μm in steps of 100 μm whilst the pulse energy and repetition rate were fixed at 1 mJ and 70 kHz, respectively. To study the effects of laser heat accumulation on drilling performance, the galvanometer hole indexing jump speeds ranged from 10 to 1600 mm/s. Next, the performance of a less common bidirectional scanning method, named here “2D interlaced”, was evaluated. By using this strategy, an identical number of holes should be omitted from the scanning toolpath in both XY lateral directions as shown in Fig. 2(a), which would be drilled later in subsequent repeat passes. Meanwhile, an infrared thermal camera (thermoIMAGER TIM 640, Micro-Epsilon) was deployed to monitor residual heat during drilling and identify its impact on hole diameter. The camera was calibrated using a thermocouple, and constant emissivity was assumed. The deviations in exit hole size were considered in assessing the drilling uniformity. Images of holes drilled at five different locations, i.e. on the edges and near the centre part of the test array on the SS substrate were captured using an optical microscope (ECLIPSE LV100NDA, Nikon) and then analysed following the procedure described by Martan et al., 2020. A total of four images (pixel size of $835 \mu\text{m} \times 700 \mu\text{m}$) containing holes were obtained from each of these locations as shown in Fig. 2(b).

3. Results and discussion

3.1. Single-hole laser drilling

The first part of this research concentrated on investigating the influence of key laser processing parameters in percussion drilling of 300 μm thick SS plates. Initially, we identified the minimum number of laser pulses required to drill through the substrate at a fixed repetition rate of 70 kHz and consequently the associated laser drilling time. Three different pulse durations were used, i.e. 240 ns, 620 ns and 1020 ns, whilst the pulse energy was varied from 0.1 to 1 mJ.

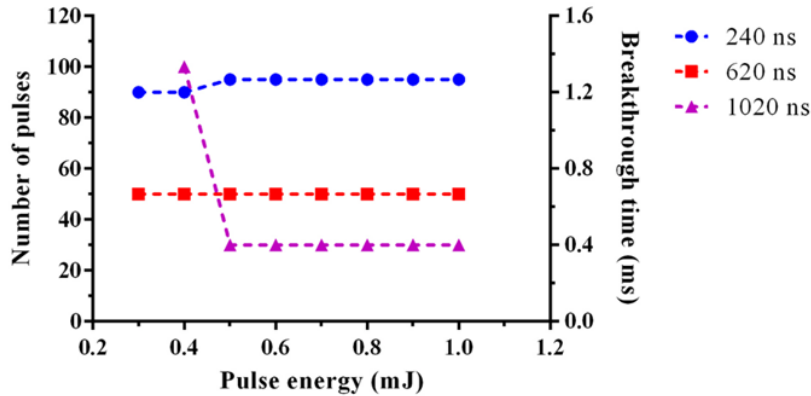


Fig. 3. The number of laser pulses and laser drill time required to breakthrough the SS substrate as a function of laser pulse energy for three different pulse durations (240 ns, 620 ns, 1020 ns).

As can be seen in Fig. 3, pulse energies up to 0.2 mJ were insufficient to penetrate the material even when the same location was irradiated with 300 consecutive laser pulses. However, drilled through holes started to appear when the laser energy was increased to 0.3 mJ and beyond up to the maximum available 1 mJ. Overall, it is evident that for a given laser pulse energy a higher number of laser pulses is required to perforate the material as the laser pulse duration decreases. This confirms that longer laser-material interactions enable faster drilling, which is in good agreement with several previous research findings on laser structuring (Banat et al., 2020). The shortest drill breakthrough time achieved with the employed laser set up was 0.4 ms/hole.

Furthermore, the evolution of hole size with laser pulse energy was investigated and the results are plotted in Fig. 4(a). The repetition rate and the number of incident laser pulses were set to 70 kHz and 100, respectively. As expected, the average hole diameter at both the entrance and exit sides increased almost linearly with the laser pulse energy. Both entry and exit hole sizes increased by more than 40% from 0.3 to 1 mJ at a pulse duration of 240 ns. Considering holes drilled with the same laser pulse energy but different laser pulse duration, it is apparent that holes with larger exit diameters were produced upon irradiation with shorter laser pulses. This was mainly attributed to their higher peak power and a more detailed explanation is provided by Rößler et al., 2020. The optical images shown as insets in Fig. 4(a) demonstrate that longer laser pulse durations had a negative impact on hole quality with more pronounced thermal effects, i.e. unwanted surface oxidation and recast layer observed on the hole exit side.

The effect of laser repetition rate on drilling efficiency was assessed using 70, 100 and 130 kHz whilst keeping all other laser processing parameters constant, i.e. laser pulse energy 0.5 mJ, laser pulse duration 240 ns and 100 incident laser pulses on target. By measuring the entrance and exit hole diameters of each hole, it was found that increasing the repetition rate leads to higher volume removal (see Fig. 4(b)). Apart from the change in hole diameter, a larger amount of recast layer was formed around the hole entrance with the increase of repetition rate, quite likely due to laser heat accumulation. At such high repetition rates, there is not sufficient time for the material to cool down to ambient temperature between successive laser pulses and thus the residual heat accumulates in the irradiated area. This is particularly true for SS that is a poor thermal conductor. This gradually raises the substrate surface temperature and can additionally cause a reduction in the ablation threshold fluence with the formation of structural defects (Martan et al., 2021). This phenomenon can explain the increase in hole diameter observed at higher repetition rates.

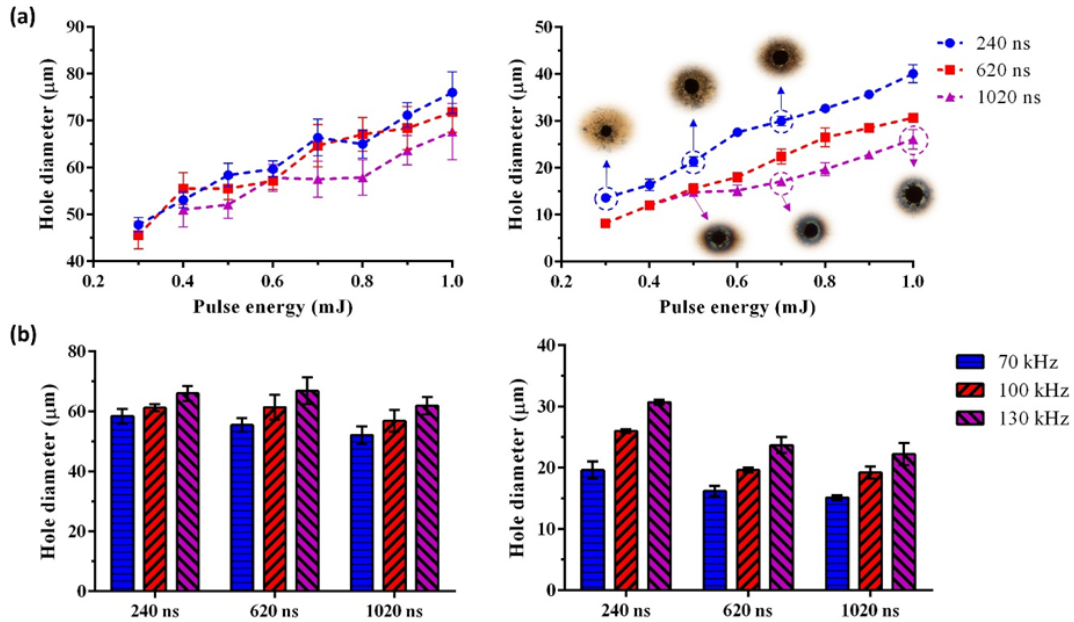


Fig. 4. Effects of two critical laser parameters on drilling performance for three different pulse durations: (a) Influence of pulse energy on entrance (left) and exit (right) diameter of holes drilled at a fixed repetition rate of 70 kHz and 100 laser pulse; (b) entrance (left) and exit (right) hole diameters for 0.5 mJ pulse energy and 100 laser pulses at varying repetition rates.

3.2. High-density hole drilling

Next, we investigated laser drilling of high-density holes over a $10 \times 10 \text{ mm}^2$ area on SS substrates. At first, the impact of pitch distance on the hole dimensional/geometrical characteristics was evaluated. Only the exit hole diameters were considered in this analysis. We initially established a baseline in our hole measurements ensuring no heat accumulation effects were present by deliberately introducing a time delay of 3sec between drilled holes. This is enough time to let the material relax to the ambient temperature after drilling. The sequential scanning method was used to drill at varying pitch distance but with constant laser pulse energy of 1 mJ and using 100 laser pulses per hole. The results obtained for the three examined pulse durations are presented in Fig. 5. As anticipated, there were no significant variations in the average exit diameter and circularity of drilled holes even for the shortest tested pitch distance of $200 \mu\text{m}$. At the same time, it is evident from Fig. 5 that nanosecond pulsed fibre lasers can produce highly circular holes, with average values better than 0.91.

Subsequently, the same experimental procedure was repeated at varying scanner jump speeds indexing between holes without applying any further time delay. Since a similar trend was observed for all the investigated laser pulse durations, results for only 620 ns are given in Fig. 6(a). If heat accumulation effects were absent, very similar measurements should be obtained to those depicted in Fig. 5. Indeed, this is partially the case for drilled holes with pitch distances larger than $300 \mu\text{m}$ as the variations in their exit diameter were almost negligible. Therefore, it can be indirectly inferred that no significant heat accumulation occurs with increasing processing speed at those (long enough) hole pitch distances. This can also be supported by the fact that the measured surface temperature 50 ms after drilling did not show any significant variations across the different examined scanner jump speeds (see Fig. 6(b)). However, this was not true when drilling holes at

tighter pitch smaller than or equal to 300 μm . A significant rise in the surface temperature around the irradiated areas followed by excessive surface oxidation was observed in that case, especially at jump speeds above 400 mm/s. This implies that laser residual heat was transferred between holes gradually accumulating on the surface and probably played some role influencing our drilling results. The considerable variations in the measured hole diameters indicate that heat accumulation had a negative impact on hole uniformity. Interestingly, as shown in Fig. 6(a), the average hole exit diameter at 200 μm pitch peaked at a jump speed of 400 mm/s before gradually decreasing. At this speed, a considerable deviation of more than 42% was measured when comparing the average diameter of these holes with the reference ones produced using the same laser conditions in the initial single-hole drilling experiments described in section 3.1.

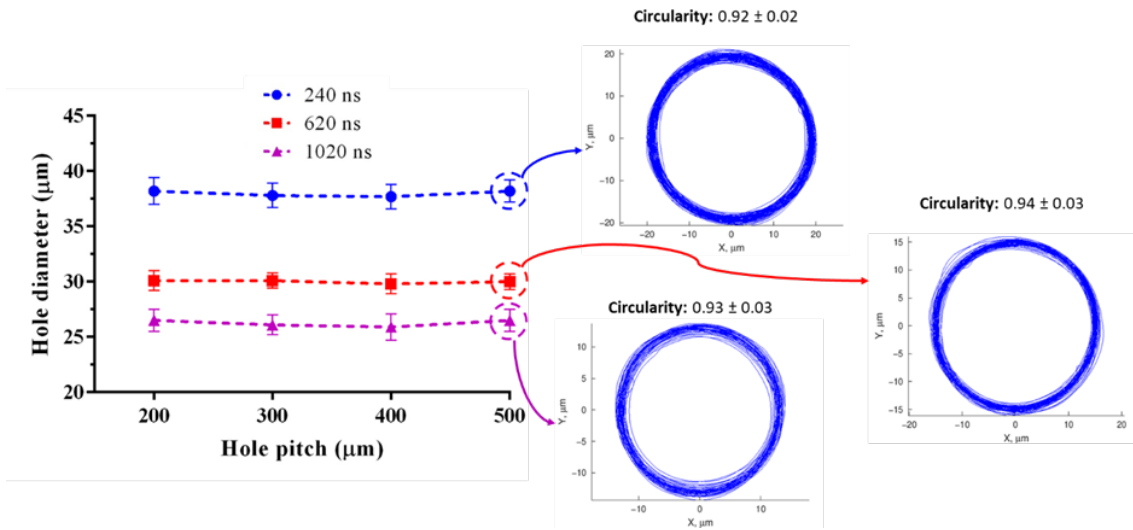


Fig. 5. The influence of hole array pitch distance on the exit hole diameter and circularity in the absence of laser heat accumulation. Laser drilling was conducted at a pulse duration, repetition rate and pulse energy of 620 ns, 70 kHz and 1 mJ, respectively.

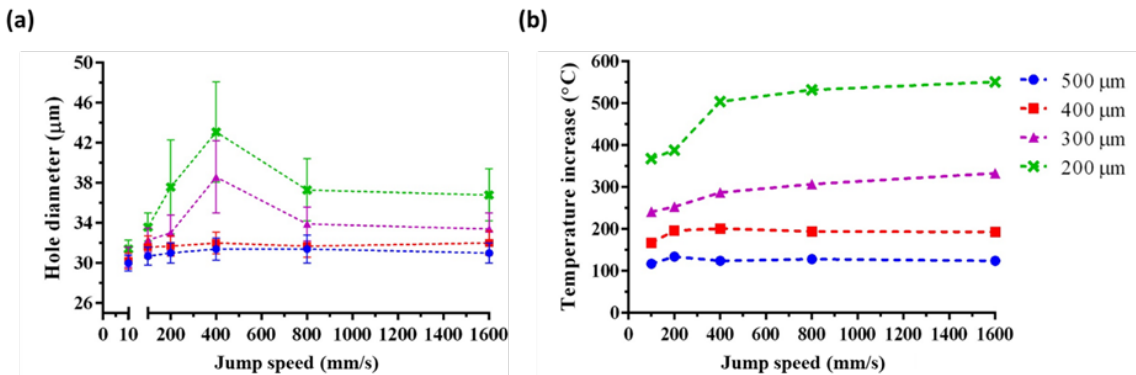


Fig. 6. The impact of scanner jump speed between drilled holes on the (a) exit hole diameter and (b) measured temperature rise of the drilled substrate for different hole pitch distances. Fixed laser parameters: 1 mJ, 70 kHz, 100 laser pulses, 620 ns.

To interpret these results, a better understanding was required of how thermal conduction between hole locations affects the drilling performance. Therefore, the distribution of laser-induced residual heat over the irradiated area and its effects on the hole size were analysed. According to the thermal image obtained from the irradiated area 50 ms after completing test drilling of 50 by 50 hole array with 200 μm pitch at speed 400 mm/s, laser residual heat in the substrate was clearly accumulated over time in the region towards the end of the drilling process, as shown in Fig. 7(a). This is not surprising. Exit hole diameters were measured at five different locations (see Fig. 2(b)), and the results are plotted in Fig. 7(b). It is evident by comparing the two images shown in Fig. 7 that larger exit hole diameters were obtained in the regions where a higher surface temperature was recorded, and hence a correlation between them exists. The higher temperatures result from both local temperature rise around the crater due to laser drilling (minus any heat escaping with the hot ablation products) as well as heat conduction from residual heat present in neighbouring drilled holes. These findings could then explain the observed reduction in average hole diameter at jump speeds above 400 mm/s as seen in Fig. 6. At 400 mm/s the indexing time between holes for 200 μm pitch is 0.5 ms assuming the scanner reaches almost instantly its commanded velocity. Thus, considering a thermal diffusivity of 3.35 mm^2/s for SS, any residual heat from the nearest preceding drilled hole would diffuse radially about 80 μm away from that region during this time. In addition, further residual heat remaining in the preceding hole vicinity, which was drilled with 100 pulses at the lowest examined laser frequency of 70 kHz, will diffuse approximately 140 μm away during the 1.4 ms drill time. The sum total diffusion distance of 220 μm is very close to the 200 μm pitch distance under discussion. This simple qualitative argument indicates that for indexing jump speeds above 400 mm/s, there is increasingly less contribution towards temperature rise at follow-up neighbouring holes due to diffused residual laser heat from other preceding drilled holes. In other words, there is not enough time for such heat to travel between hole locations. This should gradually result in smaller diameter holes with increasing further the scanner indexing speed as observed in Fig. 6(a) because more laser energy is required to drill through the SS substrate.

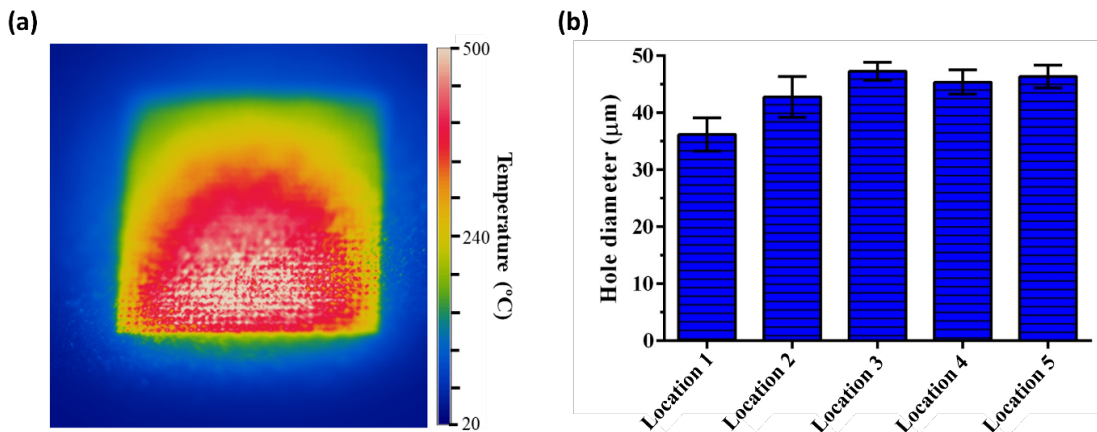


Fig. 7. Thermal imaging analysis of holes with 200 μm pitch: (a) thermal image captured 50 ms after drilling the array of holes on the SS surface at a jump speed of 400 mm/s; the respective average exit hole diameters measured from the five different locations on the substrate.

Generally, laser-induced heat accumulation side effects are unwanted in most drilling applications and thus strategies to suppress them are of great importance to enable the industrial uptake of nanosecond pulsed lasers. In this regard, the effectiveness of the 2D interlaced scanning method (2D IM) to improve the overall drilling performance was evaluated. Since thermal side effects were far more pronounced on high-density drilled holes with 200 μm pitch, the performance of this method was tested only for such holes to demonstrate the wider concept we propose here. To minimise or exclude any influence from heat accumulation while achieving as low TAKT time as possible, any two follow-up hole positions were skipped in both XY lateral directions after each drilled hole to increase momentarily the hole pitch distance in each scan. Follow-up repeat scans filled in the skipped holes always maintaining a large enough, “safe” pitch distance. As can be seen in Fig. 8, the 2D IM was more effective in dealing with residual heat accumulation compared to the previously discussed sequential method. A decrease in the average exit hole diameter was observed using the former strategy at pitch distance 200 μm , especially for jump speed of 400 mm/s. But still some deviations from the reference holes were present. Based on thermal imaging and optical microscopy analysis, these deviations were attributed to the higher surface temperature in the regions where the holes were drilled with the subsequent passes, which resulted in holes with bigger exit diameters. To counteract this phenomenon and improve the hole drilling uniformity, a simple modification on the original 2D IM was made, named here 2D IM2. The 2D IM2 method adjusted not only the intermediate pitch distance after each repeat pass but also the incident laser pulse energy. After a few optimisation cycles, holes very similar to the reference ones were achieved by properly reducing the incident laser pulse energy in the subsequent repeat passes for each hole location as shown in Fig. 8. Overall, the shortest TAKT time required to achieve highly uniform holes with an average hole diameter close to that of our reference was only 2 ms/hole. Lastly, machine learning optimisation techniques can be used in the future to eliminate the need for time-consuming and costly experimental trials, thus enabling a broader adoption of the proposed drilling strategy (McDonnell et al., 2021).

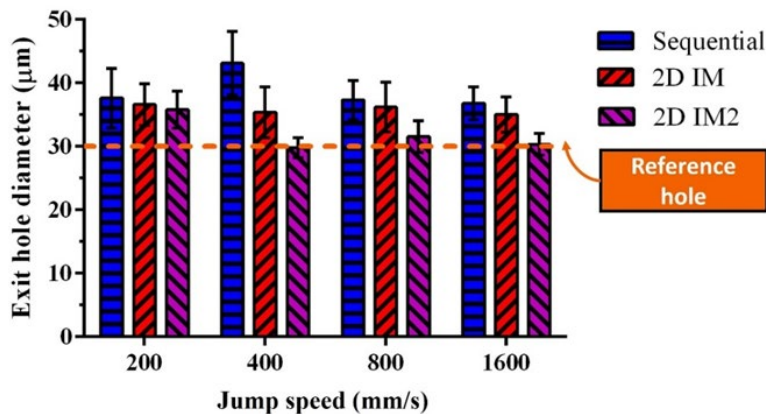


Fig. 8. Variation of average exit hole diameter as a function of indexing jump speed between holes for the three employed scanning strategies at nominal pitch distance 200 μm . The orange dashed line represents as nominal target the average exit diameter of the holes produced in the single-hole drilling experiments.

4. Conclusions

Unwanted laser-induced heat accumulation from high repetition rate nanosecond lasers can have detrimental effects in high-density industrial laser drilling. This study demonstrates a simple method to

suppress these negative side effects and hence significantly improve the overall laser drilling performance hoping to assist in their further industrial uptake. By changing the drill scanning mode from a simple sequential into a 2D interlaced method both residual heat accumulation and its negative effects on drilling uniformity were mitigated. Thermal imaging analysis revealed a strong correlation between substrate surface temperature and hole size, and thus knowing the surface temperature in advance could help to rapidly optimise the overall drilling process. In fact, tuning of laser pulse energy based on the residual surface temperature proved a versatile tool for controlling/counteracting the undesired thermal side effects induced by high-average-power nanosecond lasers. It was demonstrated that highly uniform through holes of 30 μm exit diameter could be produced in 300 μm thick SS foils. The standard deviation was only $\pm 1.7 \mu\text{m}$ and a high drilling rate of 2 ms/hole was achieved. Future efforts would be devoted to developing a semi-empirical or deep learning model for predicting the laser pulse energy required on each substrate location for uniform laser drilling.

Acknowledgements

We would like to acknowledge continuous support from Physik Instrumente (PI) GmbH.

References

- Amako, J., & Fujii, E. (2016). Beam delivery system with a non-digitized diffractive beam splitter for laser-drilling of silicon. *Optics and Lasers in Engineering*, 77, 1-7.
- Banat, D., Ganguly, S., Meco, S., & Harrison, P. (2020). Application of high power pulsed nanosecond fibre lasers in processing ultra-thin aluminium foils. *Optics and Lasers in Engineering*, 129, 106075.
- Chaubey, S. K., & Gupta, K. (2022). Developing Meso and Microholes by Spark-Erosion Based Drilling Processes: A Critical Review. *Micromachines*, 13(6), 885.
- Dondieu, S. D., Włodarczyk, K. L., Harrison, P., Rosowski, A., Gabzdyl, J., Reuben, R. L., & Hand, D. P. (2020). Process Optimization for 100 W Nanosecond Pulsed Fiber Laser Engraving of 316L Grade Stainless Steel. *Journal of Manufacturing and Materials Processing*, 4(4), 110.
- Franz, D., Häfner, T., Kunz, T., Roth, G.-L., Rung, S., Esen, C., & Hellmann, R. (2022). Ultrashort Pulsed Laser Drilling of Printed Circuit Board Materials. *Materials*, 15(11), 3932.
- Karkantonis, T., Gaddam, A., Tao, X., See, T. L., & Dimov, S. (2022). The influence of processing environment on laser-induced periodic surface structures generated with green nanosecond laser. *Surfaces and Interfaces*, 31, 102096.
- Knowles, M. R. H., Rutterford, G., Karnakis, D., & Ferguson, A. (2007). Micro-machining of metals, ceramics and polymers using nanosecond lasers. *The International Journal of Advanced Manufacturing Technology*, 33, 95-102.
- Martan, J., Moskal, D., Smeták, L., & Honner, M. (2020). Performance and Accuracy of the Shifted Laser Surface Texturing Method. *Micromachines*, 11(5), 520.
- Martan, J., Prokešová, L., Moskal, D., Ferreira de Faria, B. C., Honner, M., & Lang, V. (2021). Heat accumulation temperature measurement in ultrashort pulse laser micromachining. *International Journal of Heat and Mass Transfer*, 168, 120866.
- McDonnell, M. D. T., Arnaldo, D., Pelletier, E., Grant-Jacob, J. A., Praeger, M., Karnakis, D., Eason, R. W., & Mills, B. (2021). Machine learning for multi-dimensional optimisation and predictive visualisation of laser machining. *Journal of Intelligent Manufacturing*, 32, 1471-1483.
- Nasrollahi, V., Penchev, P., Batal, A., Le, H., Dimov, S., & Kim, K. (2020). Laser drilling with a top-hat beam of micro-scale high aspect ratio holes in silicon nitride. *Journal of Materials Processing Technology*, 281, 116636.
- Piqué, A., Auyeung, R. C. Y., Kim, H., Charipar, N. A., & Mathews, S. A. (2016). Laser 3D micro-manufacturing. *Journal of Physics D: Applied Physics*, 49(22), 223001.
- Rößler, F., Müller, M., & Streek, A. (2020). High throughput laser drilling with high power lasers using a two-dimensional polygon mirror scanner. *Journal of Laser Micro Nanoengineering*, 15(3), 220-227.
- Wang, H.-J., Chen, Q., Lin, D.-T., Zuo, F., Zhao, Z.-X., Wang, C.-Y., & Lin, H.-T. (2018). Effect of scanning pitch on nanosecond laser micro-drilling of silicon nitride ceramic. *Ceramics International*, 44(12), 14925-14928.